Veneer-aramid Composites Performances in Multilayer Armor Systems against Level III Ballistic Threat

Ananto Nugroho
Research Center for Biomass and Bioproducts, Research Organization for Life Sciences and Environment, National Research and Innovation Agency

Triastuti
Research Center for Biomass and Bioproducts, Research Organization for Life Sciences and Environment, National Research and Innovation Agency

Iman Hidayat
Research Center for Biomass and Bioproducts, Research Organization for Life Sciences and Environment, National Research and Innovation Agency

Sandi Sufiandi
Directorate for Laboratory Management, Research Facilities, and Science and Technology Park, Deputy for Research and Infrastructure, National Research and Innovation Agency

他

https://doi.org/10.5109/7342444

出版情報：Evergreen. 12 (1), pp.125-134, 2025-03. Interdisciplinary Graduate School of Engineering Sciences, Kyushu University, Japan
バージョン：

Veneer-aramid Composites Performances in Multilayer Armor Systems against Level III Ballistic Threat

Ananto Nugroho[1], Triastuti[1], Iman Hidayat[1], Sandi Sufiandi[2,3], Anne Zulfia Syahrial[4,*]

[1]Research Center for Biomass and Bioproducts, Research Organization for Life Sciences and Environment, National Research and Innovation Agency, Jl. Raya Bogor Km 46, Cibinong, 16911, Indonesia

[2]Directorate for Laboratory Management, Research Facilities, and Science and Technology Park, Deputy for Research and Infrastructure, National Research and Innovation Agency, Jl. M.H. Thamrin No.8, Menteng, Jakarta Pusat, 10340, Indonesia

[3]Research Center for Smart Mechatronics, Research Organization for Electronics and Informatics, National Research and Innovation Agency, Jl. Sangkuriang, Dago, Bandung, 40135, Indonesia

[4]Department of Metallurgy and Material Engineering, Faculty of Engineering, Universitas Indonesia, Kampus UI Depok, 16424, Indonesia

*Author to whom correspondence should be addressed:
E-mail: anne@metal.ui.ac.id

(Received June 9, 2024; Revised December 26, 2024; Accepted January 16, 2025).

Abstract: This research demonstrates the high potential of natural material composites for use as energy-absorbing layers in ballistic armor systems. The study developed ballistic panels from veneer wood modified with bacterial cellulose through a hot densification process. The results showed that densified veneer and bacterial cellulose composites can be effectively used as hybrid composite panels in conjunction with aramid fabric as an intermediate layer within Multilayer Armor Systems. Ballistic tests demonstrated that these composite panels are impervious to 7.62 mm NATO caliber bullets. Additionally, this hybrid composite excels in energy absorption by capturing ceramic fragments and projectiles, resulting in minimal trauma energy transfer. Overall, the constructed armor structure meets the level III testing criteria according to NIJ 0101.06 standards.

Keywords: hybrid, bullets, impact, energy, absorb, trauma

1. Introduction

Multilayered armor systems (MAS) have emerged as a major innovation in bulletproof protection, particularly in the form of plates inserted into bulletproof vests. Multiple layers, each with a specific function, are designed in the structure of MAS to counter high-velocity ammunition threats[1–3]. Ceramic tiles, brittle yet extremely hard, typically form the front layer of MAS. This layer absorbs the impact energy of a projectile, shattering the ceramic into small fragments that can absorb over 50% of the projectile's impact energy[4–6]. The materials used for the ceramic are usually alumina, silicon carbide, or boron carbide. Once the projectile penetrates the ceramic layer, it reaches the intermediate composite layer, which absorbs part of the projectile's kinetic energy and traps the shattered ceramic fragments [4,7,8]. This composite material consists of strong fibers such as Kevlar, UHMWPE (Ultra-High-Molecular-Weight Polyethylene), or other polymer materials. The final layer in MAS is a ductile metal plate, which serves as the last line of defense to absorb any residual kinetic energy that may remain after passing through the first two layers, ensuring that the deformation or penetration of the projectile does not reach the wearer's body[9,10]. Common materials used for this layer are stainless steel or aluminum, which can deform without breaking, thus effectively absorbing energy. According to the NIJ 0101.06 standards, this protective layer must prevent the projectile from penetrating and ensure that the depth of deformation on the clay witness (Roma Plastilina No. 1), referred to as the backface signature (BFS), does not exceed 44 mm. This criterion is critical to minimizing trauma to the wearer[11].

Researchers are investigating the development of polymer composites reinforced with lignocellulosic-based materials like natural fibers as an environmentally friendly, low-density, and cost-effective alternative to synthetic fibers. Research on ballistic protection using natural fiber-reinforced polymer composites has been underway since

2007 and continues to evolve[12]. Although the mechanical strength of natural fibers is inherently lower compared to synthetic fibers, their capacity to absorb ballistic energy can be significantly enhanced within a polymer matrix, especially when surface modifications, such as chemical treatments or coupling agents, are applied to improve interfacial bonding and optimize energy dissipation under impact[6,9,13–16]. Natural fibers and wood both exhibit the potential of lignocellulosic-based materials, as densification can enhance their mechanical strength. Hot compression and a delignification process can easily densify wood. Previous studies indicate that densified wood can achieve mechanical strength greater than that of certain metal alloys. This increase in strength is primarily attributed to the formation of hydrogen bonds between cellulose fibers[17]. Additionally, the release of water molecules in wood during the drying and densification process also influences the mechanical properties of wood fibers[18]. Research on hot compression treatment of wood reveals significant enhancements in dimensional stability, mechanical strength, surface hardness, and overall durability[19,20].

Previous research has shown that *Acetobacter xylinum* can get into the pores of wood veneer and produce cellulose that interacts with fibers, causing hydrogen bonds to form within the densified veneer[21–23]. This modification of veneer fbers involves the assembly of bacterial cellulose (BC) into the wood fibers within a culture medium, starting with partial delignification and concluding with hot compression. As a result, the mechanical strength of densified veneer significantly increases, while the modification of natural fibers with BC can strengthen the surface bonds between natural fibers and the polymer matrix[24,25]. However, information regarding the ballistic capabilities of modified wood-based materials remains limited. Previous studies have tested the ballistic resistance of single panels, which are laminated composite of densified veneer-BC bonded with resin and aramid fabric[26]. Further research is necessary to assess the potential for optimizing MAS structures.

This paper will discuss experimental testing regarding the ballistic performance of composite panel, consisting of laminated densified veneer and aramid fabric as the intermediate layer in MAS structure. We conducted the testing on hybrid and non-hybrid panel samples, utilizing Al_2O_3 ceramic tiles as the front layer and aluminum alloy plates as the back layer. The testing procedure followed NIJ 0101.06 standards for ballistic resistance level III. After testing, we measured the depth of BFS on clay behind the target to evaluate the ballistic performance of MAS samples. Although NIJ standards do not specifically address the method for measuring the energy absorbed by the clay witness behind the target, NIJ provides standardization for clay validation based on the weight of steel balls that can be used as the basis for energy calculation. In this study, the amount of energy absorbed by the protector and the energy transmitted to the back of the target were calculated using an empirical approach developed by Kim Y et al., incorporating parameters into the clay witness[27].

2. Materials and Methods

2.1 Materials

Veneer sheets produced from the rotary cutting of 15-year-old Platinum Teak *(Tectona grandis)* logs served as the raw material for the sample. The teak logs were obtained from the research plantation at the Biomass and Bioproduct Research Center – BRIN, Cibinong, West Java. We also used acetic acid bacteria, a common bacterial starter in BC production. The starter bacteria were *Acetobacter xylinum* grown in a liquid medium. These starter bacteria were purchased from Biotechno Store Collection in liquid form inside sealed bottles. This study also used woven aramid fibers, weighing 240 g/m², in conjunction with veneer layers to fabricate composite panels. The study employed a two-component epoxy resin, mixed in a 1:1 ratio of resin and hardener, as an adhesive for bonding the laminated structures. Additionally, Al_2O_3 ceramic tiles were employed as the front layer, while 5052-H34 aluminum alloy plates were utilized as the back layer to create a layered protective system.

2.2 Densified Veneers

The experimental procedure began with the delignification of 160×160 mm veneer sheets with a thickness of 2.3 mm in a 1 M NaOH solution, heated to 90°C for 90 minutes. After the delignification process, the veneer was cleaned from the NaOH solution by washing with water, followed by the in-situ assembly of BC into the veneer cavities within a culture medium. The culture medium was prepared from a mixture of boiled old coconut water, with the addition of 0.1% ammonium sulfate, 1% acetic acid, and 5% refined sugar for every liter of coconut water. The bacterial inoculation was carried out by adding 10 mL of *Acetobacter xylinum* starter once the solution had cooled to 35°C. Bacterial fermentation occurred over a period of 5 days. After the fermentation period was completed, the veneer samples were harvested, cleaned, and drained until their moisture content reached 30-35%. Subsequently, the samples were densified using a hot press machine at 135°C with gradually increasing pressure up to 10 MPa for 1 hour, followed by oven-drying for 2 hours at 70°C. Adjustment of sample size was necessary by cutting the veneer sheets into 150×150 mm dimensions.

2.3 Target Panels

The composite used as the intermediate layer in the MAS target panel was divided into two types, hybrid and non-hybrid panels. For the non-hybrid panels serving as control samples, full lamination of aramid with polychloroprene adhesive was performed to preserve the flexibility of the aramid weave structure, as shown in Fig.

1(a). Additional non-hybrid panels were fabricated using full lamination of aramid with epoxy adhesive, as shown in Fig. 1(b). Non-hybrid samples with full lamination of densified veneer-BC using epoxy adhesive were also prepared, as shown in Fig. 1(c). Meanwhile, hybrid panels were laminated using a combination of woven aramid fibers and densified veneer-BC in varying ratios, as illustrated in Fig. 1(d) and Fig. 1(e). The panel manufacturing process involved bonding between the constituent layers using epoxy adhesive through a hand lay-up technique.

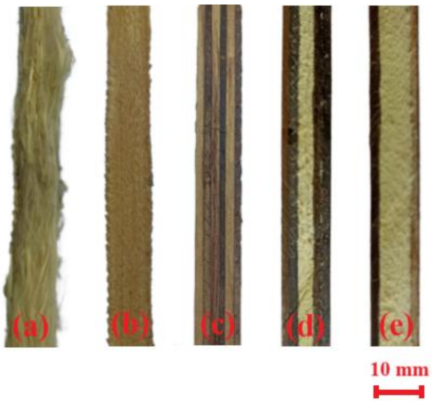

Fig. 1: Layer arrangement on the target panel (a) AP (b) AE (c) DV-BC (d) VAV1 (e) VAV2

2.4 Ballistic Testing

Subsequently, MAS target samples were prepared with the material arrangement and target position scheme illustrated in Fig. 2. Each target sample consists of a front layer made of ceramic tiles with dimensions of 50×50 mm and a thickness of 10 mm, an intermediate layer made of composite panels with dimensions of 150×150 mm and a thickness of 10 mm, and a back layer made of aluminum alloy plates with dimensions of 150×150 mm and a thickness of 5 mm. All these material layers were bonded together using a strong and flexible adhesive, polyurethane from Sikaflex. Each target sample was weighed and its areal density measured. The configuration and specifications of the MAS target samples are detailed in Table 2.

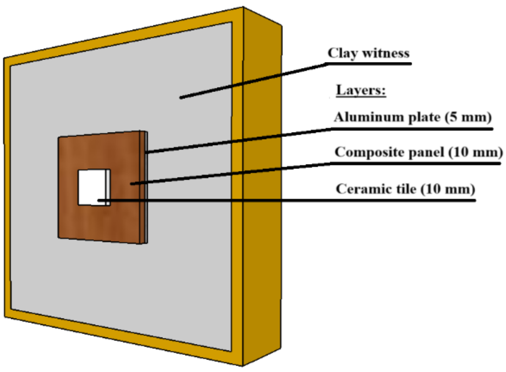

Fig. 2: Arrangement of MAS and target position during ballistic testing.

To ensure the accuracy of ballistic testing, the clay witness material must first be validated in accordance with the NIJ 0101.06 standards. This validation ensures that the clay possesses consistent mechanical properties and can accurately capture the depth of deformation caused by energy transfer during testing. The drop test validation is conducted using a steel ball with a diameter of 63.5 mm ± 0.05 mm and a weight of 1043 g ± 5 g, dropped freely from a height of 2 meters onto conditioned clay. This procedure is repeated five times, with the standard requiring the average indentation depth to be 19 mm ± 2 mm, and individual measurements not exceeding 22 mm or falling below 16 mm. As shown in Table 1, the validation results confirm that the clay witness meets these criteria, with an average indentation depth of 18.92 mm, thereby verifying its suitability for capturing backface signature (BFS) values during subsequent ballistic testing.

Ballistic testing was conducted on MAS targets, each with 6 samples, to evaluate the performance of MAS structures in withstanding bullet energy. Ballistic tests were carried out at threat level III using standard NATO 7.62 mm bullets fired from a STEYR SSG 08 rifle at a distance of 15 m from the target, following NIJ 0101.06 standard procedures. The kinetic energy of the bullets was calculated by measuring the initial projectile velocity before hitting the target using a Chronograph. The energy transmitted to the back of the target was evaluated by measuring the depth of the backface signature (BFS) indentation after impact.

Table 1. Validation results of roma plastilina No. 1 clay.

Test number	Indentation depth (mm)
1	18.70
2	18.80
3	19.50
4	18.30
5	19.30
Average	18.92

The depth of the clay indentation can be converted into a predicted steel ball impact velocity using an empirical equation[27]. The impact velocity is calculated according to Eq. 1, where v_i is the impact velocity (m/s), S_i is the clay indentation depth (mm), d is the indenter diameter (mm), and m is the identer mass (kg). This equation implies that kinetic energy is directly proportional to the indentation depth in the clay witness. With the idealization of the BFS indentation depth and the validation of the clay based on the weight of the steel ball according to NIJ standards, the energy transmitted to the clay witness can be calculated using Eq. 2, where E_k is the kinetic energy (J), and m is the mass of the steel ball (kg). Additionally, as part of the evaluation, damage mode analysis was also conducted after ballistic testing using visual imaging of the impact energy effects.

$$v_i = \sqrt[1.22]{\frac{S_i}{27.7\,(d^{-0.628})\,(m^{0.61})}} \quad (1)$$

$$E_k = \frac{1}{2}\,m v_i^{\,2} \quad (2)$$

Table 2. Specifications and configuration of the materials comprising the MAS.

MAS samples	Front layer	Intermediate layer (panels)	Back layer	Panel configuration V=veneer, A=aramid (Number of layers)	Volume ratio (aramid :veneer)	Overall thickness (mm)	Overall area density (kg/m^2)
AP	Ceramic tile	Aramid-polychloroprene	Aluminum plate	A (30)	-	22.96	61.23
AE	Ceramic tile	Aramid-epoxy	Aluminum plate	A (30)	-	25.33	65.31
DV-BC	Ceramic tile	Densified veneer BC-epoxy	Aluminum plate	V (6)	-	27.06	62.89
VAV1	Ceramic tile	Densified veneer BC-aramid-epoxy	Aluminum plate	V-A-V (2-10-2)	1:2	25.65	63.80
VAV2	Ceramic tile	Densified veneer BC-aramid-epoxy	Aluminum plate	V-A-V (1-20-1)	2:1	24.45	64.60

3. Results and Discussion

3.1 Ballistic Performance of MAS Target

From the ballistic testing results on all target samples, it was found that 7.62 mm bullets with velocities ranging from 829.97 to 866.85 m/s were unable to penetrate any type of MAS target. Penetration only occurred partially, limited to the intermediate layer of the MAS targets. The ballistic testing resulted in severe damage to the ceramic front layer, which shattered into small fragments. Figure 3 shows the visual appearance of the MAS target samples before and after ballistic testing.

In the MAS structure, the role of ceramics is crucial as it functions to absorb as much energy as possible during the initial impact, typically achieving around 50-55%[4–6]. Monteiro et al. (2015) similarly emphasized the essential function of ceramic layers in MAS, pointing out their ability to absorb a substantial amount of projectile energy through fragmentation. In line with their findings, this study noted that the fragmentation of ceramic layers in the hybrid MAS samples played a significant role in effective energy absorption, with the densified veneer-BC layer further improving the dissipation of residual kinetic energy by capturing ceramic fragments[4,6]. After impact with ceramics, the projectile erodes and undergoes deformation, making it blunter, thus reducing its kinetic energy and no longer focused. The intermediate panel layer is damaged by projectile and ceramic fragments. The fragmentation of ceramics into smaller pieces is crucial for effective energy absorption[28,29]. On the other hand, the aluminum alloy plate in the rear layer undergoes plastic deformation due to shock waves propagating from the front[30].

Fig. 3: Visual appearance of MAS target samples before and after ballistic testing (a) AP (b) AE (c) DV-BC (d) VAV1 (e) VAV2

The MAS target samples for the intermediate layer with non-hybrid material coded as AP, which serves as a control sample in common commercial protection, are shown in Fig. 3(a). Projectile fragments and ceramic fragments caused significant damage, tearing through the aramid fibers at high velocity with extensive dispersion. Although the projectile cannot fully penetrate the intermediate layer, the highly flexible aramid fibers are unable to fully absorb ballistic energy and tend to redirect it to the rear portion. This is evident from the considerable deformation on the aluminum plate at the back.

The intermediate layer with non-hybrid material coded as AE, as seen in Fig. 3(b), appears to be very robust with minimal damage due to ceramic fragments and projectile debris. However, there is slight delamination between some aramid layers indicating a small dissipation of energy due to impact. The rigidity of the second layer in the AE sample reduces its capacity to absorb impact energy. Instead, it redirects shockwave energy to the rear, as shown by the significant indentation on the aluminum layer. This rigid aramid-epoxy panel may not be able to absorb as much energy as it used to because the aramid fibers can't move as freely in response to impact energy[31].

The sample coded DV in Fig. 3(c), which is made up of a full-densified veneer-BC layer and an intermediate layer of non-hybrid material, has a bigger damage impact than the other samples. Ceramic fragments and projectile debris damage the veneer layer until it reaches the aluminum plate. Although the projectile could not penetrate the MAS structure, the veneer layer experienced extensive and deep perforation. The veneer layer's delamination suggests an attempt by the second layer to dissipate energy, but the energy was too substantial and transferred most of it to the rear layer, leading to significant deformation of the aluminum plate.

The MAS target sample for the intermediate layer with hybrid material coded as VAV1, shown in Fig. 3(d), indicates that the damage is primarily caused by compression from projectile fragments, while damage from ceramic fragments is minimal. The wood traps some ceramic fragments, preventing further damage. The projectile impact does not cause delamination within the aramid-epoxy, indicating that energy dissipation also occurs in the wood, resulting in minimal deformation of the aluminum plate.

The projectile impact damages and delaminates the aramid veneer layer at the front of the intermediate layer, coded as VAV2 in Fig. 3(e). However, the wood and aramid-epoxy layers block ceramic fragments, preventing further damage from following the delamination of the front veneer in the subsequent layers. The shockwave energy transmitted to the rear appears to be relatively small, as evidenced by the minor indentation in the aluminum plate.

3.2 Trauma Energy

The average initial velocity of the projectile measured with a chronograph was 840.17 m/s with a standard deviation of 7.32 m/s. This research used this initial velocity as a reference value to ensure consistent initial conditions across all target samples, meeting the requirements for level III ballistic testing according to NIJ 0101.06 standards[32]. From this initial velocity, it can be calculated that the initial energy of the projectile is 3335.30 J. The MAS structure effectively dissipates a portion of the energy, as indicated by the BFS measurements shown in Fig. 4, which are all below the permissible threshold of 44 mm.

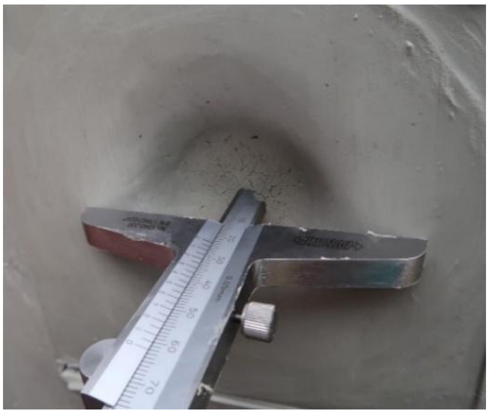

Fig. 4: Measurement of BFS on clay witnesses.

We can conclude from the recorded clay witness measurements that the average BFS depth for all samples meets the NIJ standard, as shown in Table 3. Notably, the BFS depth reveals an intriguing observation: hybrid panels, serving as intermediate layers, exhibit superior performance compared to non-hybrid panels, yielding a smaller BFS depth. Specifically, panels with aramid-polychloroprene (AP), aramid-epoxy (AE), and densified veneer-BC (DV-BC) layers have deeper BFS than panels with densified veneer-BC and aramid fabric (VAV) as intermediate layers. Consequently, the implementation of hybrid panels within the MAS structure effectively diminishes the energy transmitted to the backside, thereby reducing the trauma experienced by the wearer upon bullet impact. Despite variations in the aramid-to-veneer ratio between VAV1 and VAV2 samples, the data suggests no significant disparity in the percentage of trauma energy between them.

The BFS results show that hybrid panels perform better than non-hybrid materials in dissipating impact energy, as indicated by the shallower BFS depths in hybrid panels. This reflects their ability to reduce trauma energy transfer to the wearer. This advantage comes from the viscoelastic properties of densified veneer-BC, which improve energy absorption and distribution within the armor system. Lower trauma energy transfer means a reduced risk of internal injuries, as less kinetic energy reaches the body upon impact. This is especially important in personal protective equipment, where minimizing backface deformation and trauma energy enhances safety and survivability. Additionally, the lightweight and highenergy absorption features of hybrid panels improve comfort and mobility, making them suitable for prolonged use in demanding conditions. These findings suggest that integrating materials with such properties into intermediate layers can significantly enhance the protection offered by multilayer armor systems.

Table 3. Average BFS and trauma energy for MAS targets.

Intermediate Layer of MAS	Average BFS (mm)	Average Trauma Energy (J)	Trauma Energy (%)
AP	24.50 ± 2.45	29.47 ± 4.70	0.88 ± 0.14
AE	23.30 ± 2.49	27.16 ± 4.64	0.81 ± 0.14
DV-BC	25.28 ± 2.10	30.99 ± 4.16	0.93 ± 0.12
VAV1	21.90 ± 3.04	24.62 ± 5.78	0.74 ± 0.17
VAV2	22.00 ± 3.31	24.85 ± 5.76	0.74 ± 0.17
AP	24.50 ± 2.45	29.47 ± 4.70	0.88 ± 0.14

However, several limitations of this study must be acknowledged. The absence of dynamic imaging during ballistic testing limited our ability to observe real-time impact behavior and energy dissipation, which could provide crucial insights into material performance under high-velocity impacts. Additionally, the study used a limited number of sample configurations, which may not fully represent the variety of possible hybrid material combinations. Expanding the range of configurations and adjusting the veneer-to-aramid ratios could offer more comprehensive insights. Lastly, the manual fabrication process introduced variability in material properties, potentially affecting the consistency of the results. Standardizing production methods or adopting automated fabrication techniques could help reduce this variability in future studies.

Despite these limitations, the study's findings suggest that the improved performance of the hybrid panels can be attributed to the mechanical properties of the materials. The aramid fibers provide high tensile strength, allowing the panels to resist penetration and maintain structural integrity under high-impact forces. Meanwhile, the densified veneer-BC layer enhances energy dissipation due to its viscoelastic properties, which absorb and redistribute impact energy effectively. This combination minimizes backface deformation and reduces trauma energy transfer to the wearer, thereby improving safety and survivability. Furthermore, the ability of densified veneer-BC to capture and contain ceramic fragments contributes to the overall energy absorption and reduces secondary damage caused by projectile debris.

Because of their densified veneer-BC layers, hybrid panels excel at absorbing impact energy. The wood's ability to absorb and disperse energy relies on its viscoelastic properties, which include its viscous nature and the presence of voids. Naveen et al. (2019) also showed that hybrid laminates that include natural fibers and Kevlar displayed enhanced damping characteristics as a result of their viscoelastic properties. These results are in agreement with the findings of this study, which revealed that the densified veneer-BC layers greatly improved the energy absorption and trauma mitigation abilities of the hybrid panels. Additionally, the storage modulus and damping capacity identified in this research align with the high viscoelastic performance noted by Naveen et al. (2019), further supporting the potential of hybrid materials for ballistic applications[33)]. These characteristics help delay the impact response, thereby enhancing energy dissipation. The material's shock toughness closely links to this damping effect. These conclusions align with research conducted by Naveen et al (2019), which found that hybrid laminate composites, made from a blend of Kevlar and 25% Cocos nucifera fibers with epoxy, outperformed 100% Kevlar-epoxy composites[33)]. The study also indicated that the thermal stability of hybrid laminates is comparable to that of Kevlar-epoxy composites. Additionally, hybrid laminates exhibit higher storage modulus and loss modulus, along with superior damping properties compared to Kevlar-epoxy composites. In addition, this study discovered that the viscoelastic properties of densified veneer-BC have a high storage modulus and stiffness, which makes them better at absorbing energy[22)].

3.3 Areal Density to Trauma Energy

Despite using the same ceramic and aluminum materials, the areal density of the target samples heavily depends on the composite weight and volume within each intermediate layer of the MAS structure. Furthermore, the volume of the composite panel is significantly influenced by its material configuration and composition, particularly when densified veneer-BC layers are incorporated, which tends to increase the panel thickness. Additionally, the choice of epoxy matrix and polyurethane adhesive during the manual production process impacts the final outcome of the samples. While higher areal density generally implies greater strength, the ability to dampen impact energy is a distinct consideration. Figure 5 illustrates the relationship between total areal density and impact trauma energy across all types of intermediate layer samples within the MAS structure.

From the analysis of the relationship between areal density and trauma energy, it is evident that MAS target samples with lower areal density tend to experience higher trauma energy transfer. Even though strong synthetic aramid fibers are used, the AP intermediate layer sample with polyurethane adhesive is usually quite flexible and lacks the stiffness needed to effectively release kinetic energy. On the other hand, the AE intermediate layer sample has an aramid fiber composite with an epoxy matrix that usually has a high areal density. This is attributed to the epoxy penetrating into the fibers, making the panel stiffer, thus capable of dissipating trauma energy more effectively, resulting in smaller energy transfers.

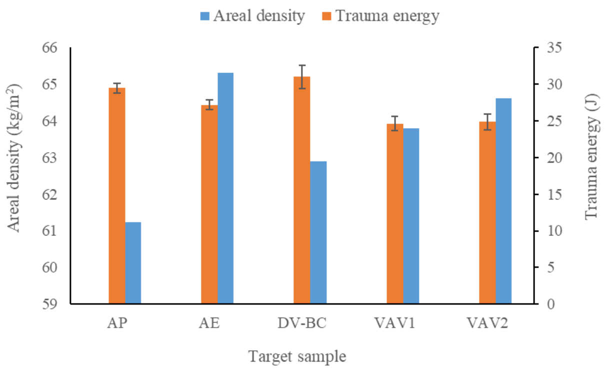

Fig. 5: The relationship between areal density and trauma energy.

On the other hand, more trauma energy is transferred in the DV-BC intermediate layer sample, which has low areal density and weak veneer strength. In contrast, the hybrid sample composed of aramid fibers and densified veneer-BC exhibits reduced transmission of trauma energy, despite its lesser weight and lower areal density compared to aramid-epoxy. This is due to the contribution of modified densified veneer wood, which has excellent damping properties and the ability to capture fragments.

3.4 Failure of MAS

Figure 6 shows the failure mode display for all types of MAS samples after ballistic testing. The test results show that the MAS structure effectively prevents projectile penetration. Damage is confined to the middle layer and the rear aluminum plate after the ceramic layer shatters. This research observes the perforation diameter, penetration depth, and sample deformation depth for each sample and damage section.

In order to assess the effectiveness of each intermediate layer panel in the MAS construction, it is crucial to examine the density, perforation diameter, penetration depth, and deformation depth of each sample. Figure 7 demonstrates that adding densified veneer-BC layers to the outside behind the ceramic tends to reduce the diameter of the perforation damage. Dispersed ceramic fragments caused broader damage, which this layer effectively mitigates.

In terms of penetration depth, aramid-epoxy samples consistently exhibit superior toughness compared to other samples. However, when assessing deformation depth from the intermediate layer to the aluminum plate due to impact energy transfer and shock wave impact, densified veneer-BC and aramid hybrid panels showcase the most effective performance. Notably, hybrid panel samples also demonstrate lighter density compared to their aramid-epoxy counterparts.

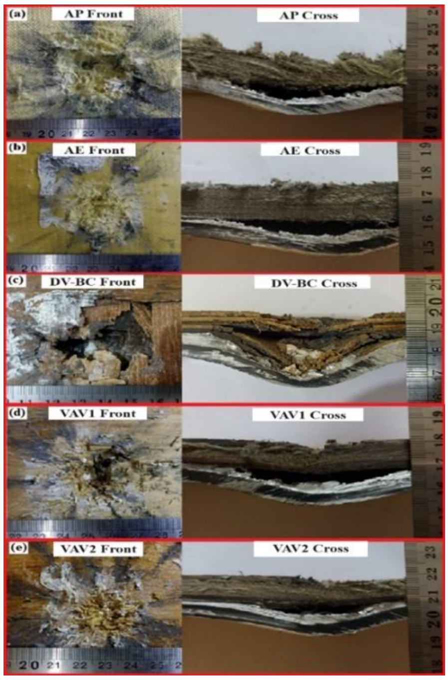

Fig. 6: Frontal view and cross-section of MAS target samples after ballistic testing (a) AP (b) AE (c) DV-BC (d) VAV1 (e) VAV2

Monteiro et al. (2015) pointed out that delamination in aramid layers is a frequent failure mode when subjected to high-velocity impacts. This study found comparable behavior in aramid-epoxy samples, where delamination led to decreased energy dissipation and greater deformation in the rear layers. In contrast, the hybrid panels examined in this study exhibited enhanced performance, as the addition of densified veneer-BC layers minimized delamination and effectively contained ceramic fragments. These results underscore the enhanced structural integrity and energy absorption capabilities of hybrid panels in comparison to conventional aramid-based designs[4].

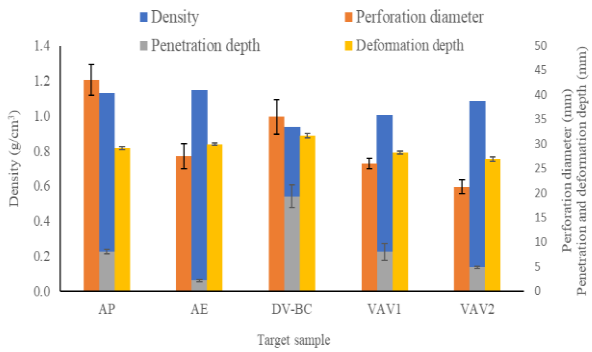

Fig. 7: Comparison of density, deformation diameter, penetration depth, and deformation depth for each intermediate layer in the MAS samples.

3.5 SEM Observations

The SEM results revealed damaged areas on both types of aramid and laminated densified veneer-BC, which serve as intermediate layers in the MAS. The primary mechanism of energy absorption and dissipation in these intermediate layer panels relates to the fibers ability to capture fragmented ceramic and shattered bullets[34–36].

In Figure 8(a), it is evident that ceramic fragments can tear through some of the aramid fibers. However, the aramid-epoxy composite successfully captures a small portion of the ceramic fragment. In Figure 8(b), the veneer wood fibers capture a significant accumulation of ceramic fragments. The fiber's strength isn't the only factor that affects its ability to catch these fragments; mechanical interlocking mechanisms, van der Waals forces, and static charges on the synthetic and natural fiber surfaces also play a role[6,37].

According to prior research by Monteiro et al., a target consisting only of a ceramic layer in the front and an aluminum alloy plate in the back, without any intermediate layer, is unable to absorb enough energy to withstand fragment explosions[4]. The same source reveals that the intermediate layer dissipates more than 36% of kinetic energy in the process of capturing ceramic fragments. Furthermore, the aluminum alloy plate absorbs even less energy, at just 7.3%. Therefore, the intermediate layer is a vital requirement to support the function of the ceramic layer.

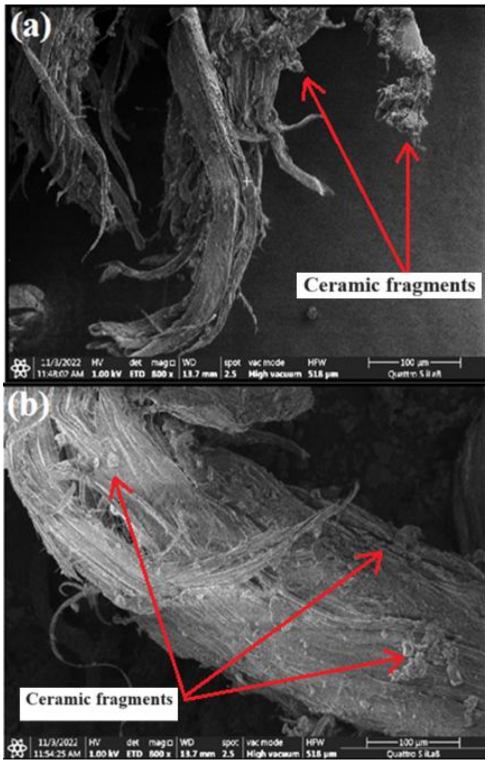

Fig. 8: Microfiber observation with SEM in the perforation damage area (a) aramid fiber (b) wood veneer fiber

4. Conclusions

Ballistic testing confirms that all MAS samples withstand 7.62 mm NATO bullets without penetration, fulfilling Level III standards as per NIJ 0101.06. Additionally, all MAS samples met the requirement of BFS values below 44 mm, thus fulfilling the Level III testing criteria according to NIJ 0101.06 standards. The intermediate layer in MAS samples, made from a hybrid composite of aramid and densified veneer-BC, exhibited better performance in reducing trauma energy compared to samples made from full aramid-epoxy. The hybrid composite has a lighter weight and a smaller area density. The densified veneer-BC composite lamination reduced the diameter of perforation damage, decreased the depth of deformation by dissipating energy, and captured ceramic fragments, thereby transferring less trauma energy to clay witnesses.

These findings underscore the potential applications of hybrid panels in real-world ballistic protection systems. Their lightweight design and effective energy absorption capabilities make them particularly suitable for personal protective equipment, such as bulletproof vests, where mobility and comfort are essential. Furthermore, their exceptional ability to reduce trauma energy and limit deformation highlights their relevance for advanced vehicle armor and protective barriers for critical infrastructure.

The observed differences in energy absorption between hybrid and non-hybrid panels present significant opportunities for further material optimization. For instance, increasing the veneer-to-aramid ratio could enhance energy dissipation while maintaining the lightweight characteristics of hybrid panels, making them more adaptable for various ballistic protection applications. Exploring alternative natural materials for the veneer layer could also improve cost efficiency and sustainability. Future research should prioritize evaluating the long-term durability of these panels under extreme operational conditions, such as high humidity or temperature fluctuations, to ensure their reliability and broader applicability.

Based on the observed data, we recommend hybrid configurations that combine densified veneer-BC with aramid fibers as an optimal solution for balancing energy absorption and weight reduction. These configurations have demonstrated lower BFS values and reduced areal density, making them ideal for lightweight ballistic protection systems. Adjusting the veneer-to-aramid ratio can further enhance energy dissipation while maintaining the structural integrity of the panels. Additionally, incorporating alternative natural materials for the veneer layer may provide cost-effective and sustainable solutions, expanding the practicality of these hybrid panels for diverse applications in personal protective equipment, vehicle armor, and protective infrastructure.

Acknowledgements

The authors express their gratitude to the Ministry of Education, Culture, Research, and Technology, the Republic of Indonesia, for providing financial support to conduct this research, under grant contract No: NKB 838/UN2.RST/HKP.05.00/2022.

References

1) F. de O. Braga, L.T. Bolzan, F.S. da Luz, P.H.L.M. Lopes, É.P. Lima, and S.N. Monteiro, "High energy ballistic and fracture comparison between multilayered armor systems using non-woven curaua fabric composites and aramid laminates," *J. Mater. Res. Technol.*, 6 (*4*) 417–422 (2017). doi:10.1016/j.jmrt.2017.08.001.
2) F.S. De Assis, A.C. Pereira, F.D.C.G. Filho, É.P. Lima, S.N. Monteiro, and R.P. Weber, "Performance of jute non-woven mat reinforced polyester matrix composite in multilayered armor," *J. Mater. Res. Technol.*, 7 (*4*) 535–540 (2018). doi:10.1016/j.jmrt.2018.05.026.
3) U.O. Costa, L.F.C. Nascimento, J.M. Garcia, S.N. Monteiro, F.S. da Luz, W.A. Pinheiro, and F. da Costa Garcia Filho, "Effect of graphene oxide coating on natural fiber composite for multilayered ballistic armor," *Polymers (Basel).*, 11 (*8*) (2019). doi:10.3390/polym11081356.
4) S.N. Monteiro, É.P. Lima, L.H.L. Louro, L.C. da Silva, and J.W. Drelich, "Unlocking function of aramid fibers in multilayered ballistic armor," *Metall. Mater. Trans. A Phys. Metall. Mater. Sci.*, 46 (*1*) 37–40 (2015). doi:10.1007/s11661-014-2678-2.
5) L.A. Rohen, F.M. Margem, S.N. Monteiro, C.M.F. Vieira, B.M. De Araujo, and E.S. Lima, "Ballistic efficiency of an individual epoxy composite reinforced with sisal fibers in multilayered armor," *Mater. Res.*, 18 55–62 (2015). doi:10.1590/1516-1439.346314.
6) S.N. Monteiro, L.H.L. Louro, W. Trindade, C.N. Elias, C.L. Ferreira, E. de Sousa Lima, R.P. Weber, J.C. Miguez Suarez, A.B.H. da Silva Figueiredo, W.A. Pinheiro, L.C. da Silva, and É.P. Lima, "Natural curaua fiber-reinforced composites in multilayered ballistic armor," *Metall. Mater. Trans. A Phys. Metall. Mater. Sci.*, 46 (*10*) 4567–4577 (2015). doi:10.1007/s11661-015-3032-z.
7) S.N. Monteiro, F. de O. Braga, E.P. Lima, L.H.L. Louro, and J.W. Drelich, "Promising curaua fiber-reinforced polyester composite for high-impact ballistic multilayered armor," *Polym. Eng. Sci.*, 57 (*9*) 947–954 (2016). doi:10.1002/pen.
8) S.N. Monteiro, F.S. de Assis, C.L. Ferreira, N.T. Simonassi, R.P. Weber, M.S. Oliveira, H.A. Colorado, and A.C. Pereira, "Fique fabric: a promising reinforcement for polymer composites," *Polymers (Basel).*, 10 (*3*) 1–10 (2018). doi:10.3390/polym10030246.
9) F.D.O. Braga, T.L. Milanezi, S.N. Monteiro, L.H.L. Louro, A.V. Gomes, and É.P. Lima, "Ballistic comparison between epoxy-ramie and epoxy-aramid composites in multilayered armor systems," *J. Mater. Res. Technol.*, 7 (*4*) 541–549 (2018). doi:10.1016/j.jmrt.2018.06.018.
10) A.C. Pereira, F.S. De Assis, F.D.C.G. Filho, M.S. Oliveira, L.C.D.C. Demosthenes, H.A.C. Lopera, and S.N. Monteiro, "Ballistic performance of multilayered armor with intermediate polyester composite reinforced with fique natural fabric and fibers," *J. Mater. Res. Technol.*, 8 (*5*) 4221–4226 (2019). doi:10.1016/j.jmrt.2019.07.031.
11) NIJ Standard-0101.06, "Ballistic Resistance of Personal Body Armor," (2008). doi:10.1017/CBO9781107415324.004.
12) Wambua P, Vangrimde B, Lomov S, Verpoest I, "The response of natural fibre composites to ballistic impact by fragment simulating projectiles," *Compos. Struct.*, 77 (*2*) 232–240 (2007). doi:10.1016/j.compstruct.2005.07.006.
13) L.F.C. Nascimento, L.I.F. Holanda, L.H.L. Louro, S.N. Monteiro, A.V. Gomes, and É.P. Lima, "Natural mallow fiber-reinforced epoxy composite for ballistic armor against class iii-a ammunition," *Metall. Mater. Trans. A Phys. Metall. Mater. Sci.*, 48 (*10*) 4425–4431 (2017). doi:10.1007/s11661-017-4264-x.
14) F.M.. S.N.L.. E.S.L.J.. E.. . Santos da Luz., "Ballistic application of coir fiber reinforced epoxy composite in multilayered armor," *Mater. Res.*, 20 23–28 (2017). doi:10.1590/1980-5373-MR-2016-0951.
15) F.C. Garcia Filho, F.S. Luz, M.S. Oliveira, W.B.A. Bezerra, J.D.V. Barbosa, and S.N. Monteiro, "Influence of rigid brazilian natural fiber arrangements in polymer composites: energy absorption and ballistic efficiency," *J. Compos. Sci.*, 5 (*8*) (2021). doi:10.3390/jcs5080201.
16) M. Karhankova, M. Adamek, L. Krstulović-Opara, V. Mach, P. Bagavac, P. Stoklasek, and A. Mizera, "Composites in ballistic applications focused on ballistic vests—a review," *J. Compos. Sci.*, 8 (*10*) 1–17 (2024). doi:10.3390/jcs8100415.
17) J. Song, C. Chen, S. Zhu, M. Zhu, J. Dai, U. Ray, Y. Li, Y. Kuang, Y. Li, N. Quispe, Y. Yao, A. Gong, U.H. Leiste, H.A. Bruck, J.Y. Zhu, A. Vellore, H. Li, M.L. Minus, Z. Jia, A. Martini, T. Li, and L. Hu, "Processing bulk natural wood into a high-performance structural material," *Nature*, 554 (*7691*) 224–228 (2018). doi:10.1038/nature25476.
18) X. Han, Y. Ye, F. Lam, J. Pu, and F. Jiang, "Hydrogen-bonding-induced assembly of aligned cellulose nanofibers into ultrastrong and tough bulk materials," *J. Mater. Chem. A*, 7 (*47*) 27023–27031 (2019). doi:10.1039/c9ta11118b.
19) P. Navi, and F. Heger, "Combined densification and thermo-hydro- mechanical processing of wood," (*May 2004*) 332–336 (2004).
20) C.H. Fang, N. Mariotti, A. Cloutier, A. Koubaa, and P. Blanchet, "Densification of wood veneers by compression combined with heat and steam," *Eur. J. Wood Wood Prod.*, 70 (*1–3*) 155–163 (2012). doi:10.1007/s00107-011-0524-4.
21) A. Nugroho, I. Hidayat, A.Z. Syahrial, and S. Sufiandi, "The Effect of Bacterial Cellulose on the

Thermo Hydro-Mechanical Treatment of Wood Veneer," in: Key Eng. Mater., Trans Tech Publications Ltd, Switzerland, 109–115 (2021). doi:10.4028/www.scientific.net/KEM.880.109.

22) A. Nugroho, Triastuti, S. Sufiandi, and A. Zulfia Syahrial, "Wood veneer reinforced with bacterial cellulose: tensile strength and dynamic mechanical analysis," *Int. J. Adv. Sci. Eng. Inf. Technol.*, 12 (*1*) 327–333 (2022). doi:10.18517/ijaseit.12.1.15139.
23) A. Nugroho, T. Triastuti, F. Akbar, S. Sufiandi, and A.Z. Syahrial, "Bacteria cellulose and resin stabilization in densified veneer," *Trends Sci.*, 20 (*4*) 6400 (2023). doi:10.48048/tis.2023.6400.
24) M. Pommet, J. Juntaro, J.Y.Y. Heng, A. Mantalaris, A.F. Lee, K. Wilson, G. Kalinka, M.S.P. Shaffer, and A. Bismarck, "Surface modification of natural fibers using bacteria: depositing bacterial cellulose onto natural fibers to create hierarchical fiber reinforced nanocomposites," *Biomacromolecules*, 9 (*6*) 1643–1651 (2008). doi:10.1021/bm800169g.
25) J. Juntaro, M. Pommet, G. Kalinka, A. Mantalaris, M.S.P. Shaffer, and A. Bismarck, "Creating hierarchical structures in renewable composites by attaching bacterial cellulose onto sisal fibers," *Adv. Mater.*, 20 (*16*) 3122–3126 (2008). doi:10.1002/adma.200703176.
26) A. Nugroho, Triastuti, S. Sufiandi, and A.Z. Syahrial, "Energy absorption of densified veneer-aramid hybrid composites subjected to ballistic impact," *Heliyon*, 8 (*8*) (2022). doi:10.1016/j.heliyon.2022.e10271.
27) Y.A. Kim, Y.S. Kim, S.H. Park, and Y.H. Kim, "Empirical and numerical study on roma plastilina #1 ballistic clay under various drop impact tests," *Mech. Adv. Mater. Struct.*, (2022). doi:10.1080/15376494.2022.2081747.
28) S.N. Monteiro, T.L. Milanezi, L.H.L. Louro, É.P. Lima, F.O. Braga, A. V Gomes, and J.W. Drelich, "Novel ballistic ramie fabric composite competing with kevlar^{TM} fabric in multilayered armor," *Mater. Des.*, 96 263–269 (2016). doi:10.1016/j.matdes.2016.02.024.
29) J.D. Hogan, L. Farbaniec, D. Mallick, V. Domnich, K. Kuwelkar, T. Sano, J.W. McCauley, and K.T. Ramesh, "Fragmentation of an advanced ceramic under ballistic impact: mechanisms and microstructure," *Int. J. Impact Eng.*, 102 47–54 (2017). doi:10.1016/j.ijimpeng.2016.12.008.
30) N. Abdulzahra, "Laser induced shock wave studies of aluminum metal," *SSRN Electron. J.*, 0–19 (2023). doi:10.2139/ssrn.4363722.
31) R. Roy, A. Majumdar, and B.S. Butola, "Comparative study of p-aramid based soft and stiff composite panels for protective application," *Fibers Polym.*, 20 (*2*) 406–412 (2019). doi:10.1007/s12221-019-8733-2.
32) E.E. Haro, A.G. Odeshi, and J.A. Szpunar, "The energy absorption behavior of hybrid composite laminates containing nano-fillers under ballistic impact," *Int. J. Impact Eng.*, 96 11–22 (2016). doi:10.1016/j.ijimpeng.2016.05.012.
33) J. Naveen, M. Jawaid, E.S. Zainudin, M.T.H. Sultan, R. Yahaya, and M.S. Abdul Majid, "Thermal degradation and viscoelastic properties of kevlar/cocos nucifera sheath reinforced epoxy hybrid composites," *Compos. Struct.*, 219 194–202 (2019). doi:10.1016/j.compstruct.2019.03.079.
34) S.N. Monteiro, J.W. Drelich, H.A.C. Lopera, L.F.C. Nascimento, F.S. da Luz, L.C. da Silva, J.L. dos Santos, F. da Costa Garcia Filho, F.S. de Assis, É.P. Lima, A.C. Pereira, N.T. Simonassi, M.S. Oliveira, L.C. da Cruz Demosthenes, U.O. Costa, R.H.M. Reis, and W.B.A. Bezerra, "Natural Fibers Reinforced Polymer Composites Applied in Ballistic Multilayered Armor for Personal Protection—An Overview," in: Miner. Met. Mater. Ser., Springer International Publishing, 33–47 (2019). doi:10.1007/978-3-030-10383-5_4.
35) F.S. da Luz, F. da C.G. Filho, M.S. Oliveira, L.F.C. Nascimento, and S.N. Monteiro, "Composites with natural fibers and conventional materials applied in a hard armor: a comparison," *Polymers (Basel).*, 12 (*9*) (2020). doi:10.3390/POLYM12091920.
36) R.H.M. Reis, L.F. Nunes, F.S. da Luz, V.S. Candido, A.C.R. da Silva, and S.N. Monteiro, "Ballistic performance of guaruman fiber composites inmultilayered armor system and as single target," *Polymers (Basel).*, 13 (*8*) 1–15 (2021). doi:10.3390/polym13081203.
37) F.S. da Luza, E.P. Lima, L.H.L. Lauro, and S.N. Monteiro, "Ballistic test of multilayered armor with intermediate epoxy composite reinforced with jute fabric," *Mater. Res.*, 18 (*2*) 170–177 (2015). doi: 10.1590/1516-1439.358914.